State of Knowledge Report

State of Knowledge on Hyperspectral Imaging Applied to Roots, Tubers and Cooking Bananas

High-throughput phenotyping protocols (HTPP) - Work Package 3

Montpellier, France, 2019

Karima MEGHAR, Centre de Coopération Internationale en Recherche Agronomique pour le Développement (CIRAD), Montpellier, France

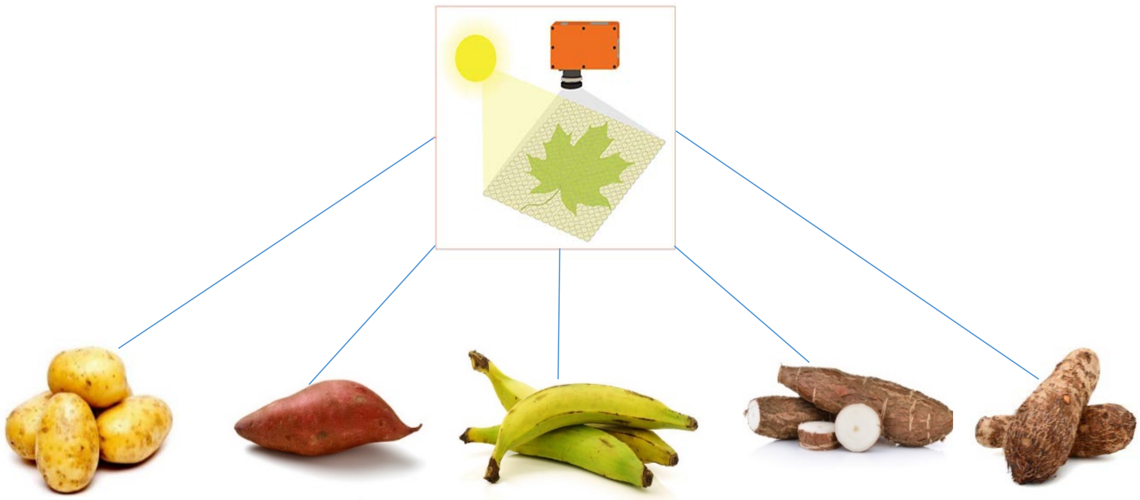

This report has been written in the framework of RTBfoods project.

To be cited as:

Karima MEGHAR, (2020*). State of Knowledge on Hyperspectral Imaging Applied to Roots, Tubers and Cooking Bananas. High-throughput phenotyping protocols (HTPP) - Work Package 3*. Montpellier, France: RTBfoods State of Knowledge Report, 23 p. https://doi.org/10.18167/agritrop/00740

Ethics: The activities, which led to the production of this manual, were assessed and approved by the CIRAD Ethics Committee (H2020 ethics self-assessment procedure). When relevant, samples were prepared according to good hygiene and manufacturing practices. When external participants were involved in an activity, they were priorly informed about the objective of the activity and explained that their participation was entirely voluntary, that they could stop the interview at any point and that their responses would be anonymous and securely stored by the research team for research purposes. Written consent (signature) was systematically sought from sensory panelists and from consumers participating in activities.

Acknowledgments: This work was supported by the RTBfoods project https://rtbfoods.cirad.fr, through a grant OPP1178942: Breeding RTB products for end user preferences (RTBfoods), to the French Agricultural Research Centre for International Development (CIRAD), Montpellier, France, by the Bill & Melinda Gates Foundation (BMGF).

CONTENTS

Table of contents

Abstract 4
1 Quality attributes characterized by hyperspectral imaging 6
2 Results and Applications 11
2.1 Potato 11
2.1.1 Biochemical constituents and physical properties 11
2.1.2 Internal and external defects 14
2.2 Banana 16
2.2.1 Chemical constituents and physical proprieties 16
2.2.2 Defects and diseases 17
2.3 Cassava 17
3 Conclusion 17
4 References 19

ABSTRACT

The objective of the RTBfoods project is to pinpoint the quality traits that determine the adoption of root, tuber and banana (RTB) varieties developed by breeders according to consumer and farmer preferences.

The aim of work package 3 (WP3) of the RTBfoods project is to develop high throughput phenotyping protocols, mainly Near Infrared Spectroscopy (NIRS), that could be applied in national and international breeding programs, postharvest processing and quality control procedures. This paper reviews research progress on hyperspectral imaging applied to RTB product characterization. This characterization may concern the quantification of different biochemical constituents, the measurement of physical properties and/or the internal and external defects.

This literature review is based on a selection of papers found through Scopus, Science Direct, Web of Science and Google Scholar. The search formula used was HSI OR and Cassava (And Yam) (And Banana) (And Potato) (And Sweet Potato) (And Root) OR tuber.

According to these requests, 48 references were found (**Annex 1**); these papers were published in different scientific journals between 2004 and 2018. Prior to 2010, the number of published articles was quite low (1) and stable (Fig. 1). The number of references increased after 2010 with a maximum of 12 publications in 2016. After 2016, the number of publications fell to 6, and 8 articles were published in 2018 for the 5 crops.

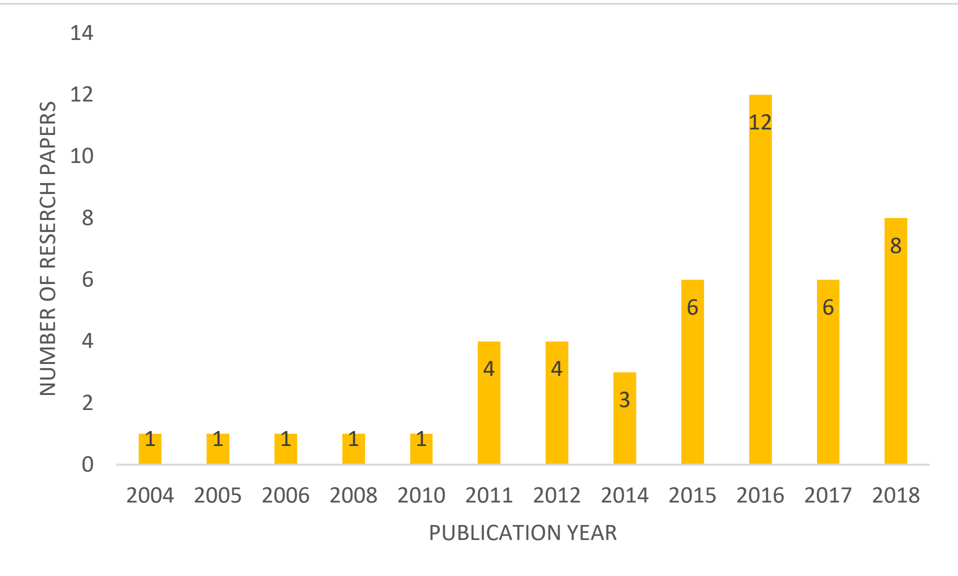

Figure 1 : *Number of references per year relating to characterization of cassava, yam, banana, sweet potato and potato using hyperspectral imaging.*

Most of the publications (85 %) concern potatoes and potato products (Fig.2). Over this period, only 11 % of scientific research on HSI techniques focused on the banana, and 2 % related both sweet potatoes and cassava.

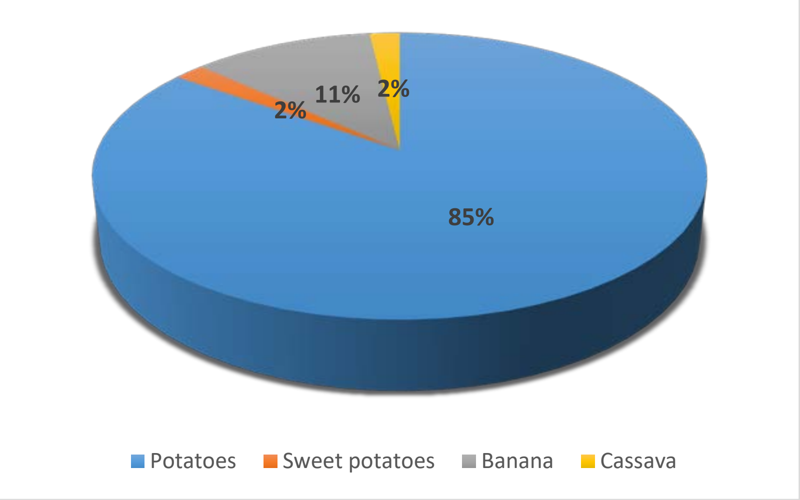

Figure 2: percentage of publications relating to potatoes, sweet potatoes, banana and cassava (period: 2004-2018).

Key Words: state of knowledge, RTB, hyperspectral camera, imaging, high-throughput protocols

1 QUALITY ATTRIBUTES CHARACTERIZED BY HYPERSPECTRAL IMAGING

The work that has been done in the selected articles on each product is summarized according to the analytical techniques used, the sample preparation procedure, the chemometric methods applied and the results obtained (Table 1).

Regarding fresh and processed potatoes, sweet potatoes, banana and cassava, most HSI investigations report quantification of the biochemical constituents. These constituents are moisture content, nitrogen stress, sugars, solid soluble, volatile compounds, water binding, dry matter, starch, acrylamide, protein, chlorophyll, water stress, soluble sugar and amino acid.

Some of the papers concern internal and external defects such as black spot, scab detection, late blight sugar-end growth defect, bud and green rind, hollow heart, crop hail damage, bruising and brown streak disease.

Another part concerns physical proprieties such as specific gravity, cooking time, clods detection, irregular potato, weight, shape and firmness. The majority of applications are based on VIS-NIR spectroscopy in diffuse reflectance, and the principal chemometrics methods selected and applied are PLS (31%) and SVM (13%) for quantification and classification respectively. As mentioned above, much of the research used HSI fresh (intact, peeled and sliced) and processed potato (dried and chips).

Table 1 : Summary of hyperspectral imaging for the quality evaluation of RTB crops and products

Crop	Acquisition mode	Product	Product processing	Quality traits	spectral range	chemometrics	Results	Reference
Potato	Reflectance	potato	slices	moisture content, chromacity	500-1000 nm	PLS, MCUVE, CARS-PLS	RMSE=0.16-0.36/0.61-1.78	(Amjad et al., 2018)
	Reflectance	potato	Manual bruising	Blackspot	400-1000 nm, 1000-2500 nm	PCA, SIMCA and PLS-DA	98.56 vs. 95.46% CC	(López-Maestresalas et al., 2016)
	Reflectance	potato	Boiled	Cooking time	400-1000 nm	PLSDA	Less than 10 % relative error	(Nguyen Do Trong et al., 2011)
	Reflectance	potato leaf		Nitrogen stress	VIS/NIRS	PLS	RMSEV=0.14 %	(Nigon et al., 2015)
	Transmittance/interactance	potato	whole tuber and slices	constituents of potato (glucose, sucrose, specific gravity, primordial leaf count and soluble solids	NIR and visible/NIR (446-1125 nm)	PLSR	______	(Rady et al., 2014)
	Reflectance	organic potato and non-organic potato		Moisture level, visual authentication	897-941 nm and 944-1678 nm	PCA, PLSDA et MC-PLSDA	Organic potato 100% accuracy of classification , moisture level PLSDA, RMSEP=<0.532	(Su and Sun, 2016a)
	Reflectance	potato	Slices	volatile compounds, cooking degree	900-1700 nm	PLSR, TBPANN		(Su and Sun, 2016b)
	Reflectance	tuber	Slices	water binding capacity (WBC) and specific gravity (SG)	897–961 nm and 1658–1753 nm	PLSR, locally weighted principal component regression (LWPCR), genetic algorithm (GA)	WBC: RMSEP=0.199 SG: RMSEP =0.009	(Su and Sun, 2016c)
	Reflectance	potato and sweet potato	Slices	Dry matter (DMC) and starch (SC) concentration		MLR, PLSR, locally weighted partial least squares regression (LWPLSR)	RMSEV: SC=0.015, DMC=0.014	(Su and Sun, 2017)

Crop	Acquisition mode	Product	Product processing	Quality traits	spectral range	chemometrics	Results	Reference
Potato	Reflectance	potato leaves	Intact leaves	Water content	862.9-1704.2 nm	correlation analysis (CA) and competitive adaptive reweighted sampling (CARS), CARS-PLSR	validation accuracy coefficient was 0.9366.	(Sun et al., 2018)
	Fluorescence	potato chips	intact chips	Acrylamide		SVM	98.33%	(Yadav et al., 2018)
	RGB	potato	______	Classification(clods)	480 nm	LDA	98 % accuracy	(Al-Mallahi et al., 2008)
	Reflectance	potato	______	detect potato tuber on potato harvester (clods)	UV(350 nm)	segmentation algorithm	98.28% of clods were detected	(Al-Mallahi et al., 2010)
	Reflectance and Transmittance	potato leaf	______	Protein and chlorophyll	400-2500 nm and 1000-2500 nm	______	______	(Botha et al., 2006)
	Reflectance	intact potato	______	Scab detection	900-1700 nm	SVM, Random Forest	97.1 % accuracy(SVM)+CFS method (1300 nm, 1303 nm, 1336 nm, 1339 nm, 1342 nm and 1503 nm)	(Dacal-Nieto et al., 2011)
	Reflectance	potato leaf	potato leaf	late blight (Phytophthora infestans)	450-900 nm	______	near 490, 530 and 670 nm) are better for classification	(Franceschini et al., 2017)
	Transmittance	potato	potato leaf	black heart and weight	400-1000 nm	PLSDA, PLS	black heart accuracy is 100%, Weight (Rp) = 0.99, and (RMSEP) = 10.88 g (9 variables)	(Gao et al., 2012)
	Reflectance	potato	potato leaf	Water stress	869-1298 cm^{-1}	______		(Gerhards et al., 2016)
	Reflectance	potato	peeled potato	Sugar-End growth defect	1100-1700 nm	______	91.7 % accuracy of classification	(Groinig et al.)
	Reflectance	potato	potato leaves	potato late blight	374-1018 nm	LS-SVM	94.87 % accuracy	(Hu et al., 2016)
	Transmittance	______	intact potato	external defects (bud and green rind) and internal defect (hollow heart)	390-1040 nm	supervised locally linear embedding (SLLE)+LSSVM	bud, green rind and hollow heart potato reached 96.83%, 86.96%, 86.96% and 95%	(Huang et al., 2015)

Crop	Acquisition mode	Product	Product processing	Quality traits	spectral range	chemometrics	Results	Reference
Potato	semi-transmission	potato		Hollow heart	390-1 040 nm	SVM, CARS, artificial fish swarm algorithm (AFSA)	Accuracy: CARS-SPA (94.64%) and AFSA-SVM (100 %)	(HUANG et al., 2015)
	______	potato		disease detection		SVM	95 % of accuracy	(Islam et al., 2017)
	Reflectance	potato	potato	multiple defects	390-1040 nm	Diffusion map and extreme learning machine DM-ELM)	sprouting potatoes, green rind potatoes, blackheart potatoes and normal potatoes respectively reached 97.30%, 93.55%, 94.44% and 100%,	(Jin et al., 2015)
	Reflectance	potato	intact potato and cylinder	Starch, soluble sugar, amino acids	380-925 nm and 400-1040 nm	PLSR	amino-acid HS-full and HS-part registered R2 values of 0.70 and 0.54 starch: HS-full and HS-part registered R^2 values in the ranges of 0.66–0.71 and 0.31–0.42, respectively sugars: HS-full and HS-part registered R2 values in the ranges of 0.19–0.20 and 0.33–0.40,	(Kjær et al., 2016)
	Reflectance	potato	peeled potato	Glycoalkaloids and Chlorophyll	UV-a, UV-b or UV-c	______	ChlR2 = 0.92, TGA, R2=0.21	(Kjær et al., 2017)
		sweet potato	purple-fleshed sweet potato	Anthocyanin content	371–1023 nm	PLSR, LS-SVM, MLR	best results with MLR (ten variables)(R2P RP2)=0.866	(Liu et al., 2017)
	Reflectance		Raw French fries	Latent defects and diseases	400-900nm	support vector classifier (The fisher linear discriminant classifier (fisherc)	varied from 99.1 % for Asterix to 93.9 %	(Noordam et al., 2005)
	______	sweet potato	drying sweet potato	the moisture content and color changes during drying	and laser-induced backscattering imaging (LLBI)	PCA, PLS	Moisture: R2=0.718 SECV=0.175, Lightness (L*): R2=0.672 SECV=6.545, Redness (a*)=: R2=0.758 SECV=4.322, Yellowness: R2=0.462, SECV=3.281	(Onwude et al., 2018)

	Acquisition	Product	Product processing	Quality traits	Spectral range	chemometrics	Results	Reference
	Reflectance	potato	two cultivars RN and FL, fresh use and chipping potato cultivars.	glucose and sucrose		PLSR, KNN, PLSDA	PLS: glucose (RN: R2=0.97 and RMSEP=3.58, FL: R2=0.81, RMSEP=1.70) sucrose: FL: R=0.60 and RPD=1.14, RN: R=0.38, RPD=1.00, classification: glucose misclassification errors of 14 % and 18 % for FL and RN, sucrose indicating lower accuracy for this sugar (34 and 30 % for FL and RN).	(Rady et al., 2015)
	multi-angular reflectance	leaf potato	potato crop	improvement leaf area index (LAI) and leaf chlorophyll content (LCC)	VIS/NIRS	PROSAIL model	RMSE from 0.70 to 0.65 m2/m2 for estimating LAI, and from 17.35 to 17.29 µg/cm2 for estimating LCC	(Roosjen et al., 2018)
	Reflectance	Purple-Fleshed Sweet Potato	slices potato	Water content, and Freezable Water Content	371–1023 nm	PLSR	(RP2) of 0.9837 and 0.9323 for moisture content and freezable water content, respectively	(Sun et al., 2017)
	Machine vision system		potato	Weight and shape of potato		MLR, PCA	Weight: The distinguished accuracy were respectively 90%, 100%, 90% for large, medium and small sizes in potato sample. Size: approximation ellipsoid and approximation spherical were 83.3% and 89.3% respectively.	(Wang et al., 2016)
	Reflectance	potato	intact potato	Bruising	400-1000 nm	______	Reached 87.88% accuracy	(Ye et al., 2018)
Banana	Reflectance	Banana	dried banana	Moisture, texture and color	400-1000 nm	PLSR	water: RMSEP=0.05 kg water/kg DM), color, b (RMSEP=1.95), texture (R2P=0.66, RMSEP=11.8)	(Nguyen-Do-Trong et al., 2018)
	Reflectance	Banana	Intact banana	moisture content, firmness and total solid solub	400-1000 nm	MLR, PLS, PCA	R2=0.85, 0.87, and 0.91 for total soluble solids, moisture and firmness of the banana fruits,	(Rajkumar et al., 2012)
	Reflectance	Banana	Intact banana	color and firmness	380-1023 nm	PLS	RPD: L∗= 2.234, a∗=6.098, b∗=2.119 and firmness=2.062,	(Xie et al., 2018)
	Reflectance	Banana	Intact banana	Browning level (shelf-life)	400-1100 nm	PCA, back propagation (BP)	Best classification rates of 95.6 % for training set and 90.5 % for testing set.	(Wang et al., 2015)

2 RESULTS AND APPLICATIONS

In this part, we discuss the main results found in the literature about application of hyperspectral imaging for high throughput phenotyping of RTB and RTB products.

2.1 Potato

2.1.1 Biochemical constituents and physical properties

Sun et al., 2017 demonstrated the potential of HSI and chemometrics methods for predicting moisture content and freezable water content, during drying process of sweet potato slices. Hyperspectral images were obtained by reflectance in VIS-NIR, and the corresponding mean spectra were extracted. Two linear calibration algorithms, known as PLSR and multiple linear regression (MLR), and a non-linear calibration algorithm known as back propagation (BP) neural network were used to establish models. Comparing the PLSR model with MSC pre-treatment presented better results with coefficients of determination for prediction (R^2P) of 0.9837 % and 0.9323 % for moisture content and freezable water content, respectively. ***Su and Sun, 2017a*** developed models for DM and starch quantification with an accuracy expressed as (R^2P=0.985, RMSEP= 0.016 %) and R^2P=0.983, RMSEP =0.015), respectively. These models based on locally weighted partial least squares regression (LWPLSR) were developed on slice samples using an InGaAs (Indium Gallium Arsenide) camera (Xeva 992, Xenics Infrared Solutions, Belgium). Furthermore, the time series variations of DMC and SC on tuber samples were visualized based on an equation to apply the simplest models to the spectral images. ***Amjad et al., 2018*** developed a model for determination of moisture content in potato slices with three thicknesses (5 mm, 7 mm, 9 mm), during a dying process (50 °C, 60 °C, 70 °C). The best model (R2= 0.93-0.98, RMSEP= 0.16-0.36 %) was obtained by using PLS method in spectral range of 400-1000 nm and an imager (ImSpector V10E, Specim Spectral Imaging Ltd., Finland). ***(Botha et al., 2006)*** evaluated the ability of the PROSPECT model to estimate leaf chlorophyll and protein contents of two contrasting potato cultivars during two growing seasons, using the ASD FieldSpec Pro FR spectroradiometer (Boulder, CO) in a spectral range of 250-2500 nm. They conclude that the chlorophyll predicted with a low accuracy (R2= 0.32-0.53, RMSEP= 4.53-5.33 µg cm^{-2}) was probably related to sample variability induced by prolonged drought conditions, and protein content could not be predicted with any degree of accuracy by the model (R^2= 0.00-0.01, RMSEP= 0.0020-0.0041 mg.cm-^{2}). Then in the paper of ***Gerhards et al., 2016*** the HyperCam-LW HIS camera (Telops Inc., Quebec, Canada) was used to measure water stress of 60 potato plants with one half of the plants watered and the other half stressed. No striking differences were apparent for hyperspectral and broadband TIR imagers in deriving accurate leaf temperatures (5) among the temperature based measurements.

Kjær et al., 2016 evaluated the potential use of HSI in potato assessment and sorting. For this purpose, 60 samples of potatoes of 10 different cultivars analysed by hyperspectral camera with an ImSpector V10 spectrograph (Specim, Finland) in the spectral range 380-1050 nm. The samples were analysed with two different methods, the first on intact potato (HS-full) and the second on cylindrical pieces (HS-part) for prediction of density, DM, starch, amino-acid, soluble sugars and conductivity. For density, DM and starch the results from the two methodologies, HS-full and HS-part, registered R^2=0.66–0.71 and 0.31–0.42, respectively. Concerning the prediction of soluble sugars HS-full and HS-part registered R^2 values in the ranges of 0.19–0.20 and 0.33–0.40, respectively, for the reducing sugars glucose, fructose, 0.41, and 0.31, respectively. Results from all the methods HS-full, HS-part, R2=0.45, 0.23 respectively. ***Kjær et al. 2017*** also investigated the use of HSI to detect and quantify chlorophyll (Chl) and total glycoalkaloid in potatoes. Four varieties were wounded or treated with red, blue, red/blue, UV-a, UV-b or UV-c light. The results showed that the HSI system predicted the concentrations of Chl with a relatively high degree of accuracy, and a prediction R^2=0.92. Prediction of TGA was not satisfactory, with R^2= 0.21. The study of ***(Liu et al., 2017)*** aimed to investigate the potential of HSI for prediction of anthocyanin content within purple-fleshed sweet potato (PFSP) during the drying process. Three algorithms including PLSR, LS-SVM, and multiple linear regression (MLR) were used to build models based on ten optimal wavelengths selected in the spectral range of 371-1023 nm. The best results were obtained with RC-MLR with R^2p=0.87. The visualization of anthocyanin during the drying process cannot be achieved by those methods.

(Nguyen Do Trong et al., 2011) demonstrated the potential of HSI in the wavelength range 400-1000 nm to detect the optimum cooking time (CT) of potatoes using an ImSpector V10 spectrograph (Spectral Imaging Ltd., Oulu, Finland). For this purpose, 33 samples were bought in the market. The samples were scanned at 3, 6, 9, 12, 15, 18, 21, 24, 27 and 30 mins cooking time. The supervised method of classification PLSDA was employed to discriminate between the pixel spectra for the cooked regions, and those for the remaining raw regions. In this study the cooked and raw parts of boiled potatoes were discriminated successfully; the optimal cooking time could be predicted with less than 10 % relative error. ***Su and Sun, 2016*** also investigated the potential feasibility of using hyperspectral imaging (900–1700 nm) for predicting cooking degree (TCD) and the volatility of tuber compositions (VTC) in low temperature baking (LTB). To do this, they used six tuber categories from different origins. The tuber slices were cooked by LTB for five time periods including 40, 80, 120, 190, and 260 mins; for each time, the samples were scanned by HSI. The partial least squares regression (PLSR) and three-layer back propagation artificial neural network (TBPANN) models were established to predict VTC and TCD using the entire spectral range and the feature wavelengths. The optimal combination of characteristic wavelengths was 991, 1031, 1071, 1138, 1252, 1403, 1460 and 1641 nm. The best model was obtained by the FMCIA-TBPANN approach (R^2 =0.967 and RMSEP=0.307 mins).

The objective of the study of ***Nigon et al., 2014*** was to evaluate the implications of using high spatial resolution broad-band imagery for determining Nitrogen (N) prescriptions at different growth stages of potatoes. Aerial images were obtained for research plots, as well as for a commercial potato field (59 ha) near Becker, Minnesota on 30, 56 and 79 days after emergence (DAE) with a multispectral camera (AEROCam, Grand Forks, ND, USA). Five N treatments with varying rates and timing of N fertilizer, and two potato varieties were used. N stress based on leaf N concentration was predicted adequately within dates (R^2= 0.49 to 0.82). One year later, ***Nigon et al***. evaluated the ability of HSI to predict N stress in potatoes (Solanum tuberosum) during two growing seasons (2010 and 2011). For this purpose, five N treatments with varying rates and timing of N fertilizer were applied, on two potato cultivars, Russet Burbank (RB) and Alpine Russet (AR). The hyperspectral reflectance images were acquired with an (AISA Eagle) visible/near (401-982 nm) infrared hyperspectral imaging sensor (SPECIM, Spectral Imaging Ltd., Oulu, Finland). The best PLS models predicted N concentration R^2 = 0.79, RMSECV = 14% across dates for RB; R^2 = 0.77, RMSECV = 13% across dates for AR.

Rady et al., 2014a demonstrated the possibility of rapid prediction of the glucose and sucrose in two fresh potato cultivars using VIS-NIR hyperspectral reflectance imaging. The samples were cut uniformly into slices 12.7 mm thick. PLSR, feed forward neural networks (FFNN), radial basis functions neural networks (RBFNN), and exact design radial basis functions (RBFNNE) neural networks were used for building calibration and prediction models. The results showed a strong correlation for glucose for Russet Norkotah (RN) with R =0.97; whereas those values= 0.81 for Frito Lay (FL). Sucrose models showed less correlation performance with R= 0.60 for FL, and 0.38 for RN. The K-nearest neighbor (Knn) and partial least squares discriminant analysis (PLSDA) results were glucose misclassification errors of 14 % and 18 % for FL and RN, respectively. However, classification errors were higher for sucrose, indicating lower accuracy for this sugar (34 and 30 % for FL and RN)***. Rady et al., 2014b*** also used visible/NIR HSI to determine glucose, sucrose, specific gravity, primordial leaf count, and soluble solids of (FL) (chipping) and Russet Norkotah (RN) (table) potato cultivars. The hyperspectral images for the whole and sliced samples were acquired in the range 400-1000 nm using hyperspectral reflectance mode within a Hamamatsu dual mode cooled CCD camera (model No. C4880, Hamamatsu Photonics, Hamamatsu, Japan). PLSR was used to obtain the prediction models; the optimum model for leaf counts and glucose were obtained for leaf count from interactance with sliced samples resulting in R (RPD) = 0.95(3.29) for FL, and 0.90(2.19) for RN. For glucose, interactance also yielded the best model with R (RPD) =0.90(2.14) for FL, and 0.95(3.12) for R. The best performance for soluble solids for FL with R (RPD) = 0.55(1.18). Also, for sucrose = 0.81(1.63) for FL from sliced samples, and 0.81(1.64) whole tubers. Poorer performances were obtained with transmittance mode.

Roosjen et al., 2016 described an innovative and fast method using a hyperspectral pushbroom spectrometer mounted on a multirotor unmanned aerial vehicle (UAV) to perform such multi-angular measurements. They used this method to study the reflectance anisotropy of the potato at different growth stages, with a Rahman-Pinty-Verstraete (RPV) model in the 450–915 nm range. The UAV measurements were performed using the Wageningen UR Hyperspectral Mapping system (HYMSY) on board an Altura AT8 octocopter. The results of this study indicate that the presented method is capable of retrieving anisotropic reflectance characteristics of vegetation canopies, and that it is a feasible alternative for field goniometer measurements.

The discrimination of organic potato (OP) and identification of tuber moisture levels were investigated by ***Su and Sun, 2016b*** on sliced tuber samples and dehydrated in an oven under the temperature of 80 ± 2 °C for six time periods of 0, 30, 60, 90, 150, and 210 mins. The images were acquired using a Specim ImSpector N17E spectrograph (Spectral Imaging Ltd., Oulu, Finland) covering an NIR range of 897–1753 nm. They concluded that has a great potential for discrimination of OP and identification of tuber moisture levels using PLSDA models. The OP samples were identified correctly (100% accuracy) from non-organic tubers, R^2P= 0.979 and RMSEP ≤0.532. For tuber moisture levels, in the results obtained were correct classification of ≥91.6 %.

In order to indicate potato crop water content and guide precision irrigation, ***Sun et al., 2018*** developed a competitive adaptive reweighted sampling PLS model (CARS-PLS) to predict the leaves water content, with a calibration accuracy of 99 % and validation accuracy of 94 %. The spectral reflectance of 355 samples was collected by hyperspectral camera (i2D CCD array, detector (LT365), spectrometer (V10E), uniform light source), in the range of 862.9-1704.2 nm. Detection of acrylamide in fried potato chips using continuous wavelet transform was determined by ***Yadav et al., 2018.*** An 8 mega-pixels digital camera was used in the proposed work to capture the image of potato slices. The potato chip area was segmented from its background by extraction of discriminatory features in the continuous wavelet transform domain using Morlet wavelet. The discriminatory features were analyzed by the Support Vector Machine classifier (SVM). The results registered a good accuracy of 98.33% with 100% specificity. In order to improve the precision of dry matter content determination in potatoes by HSI technology, ***Zhu et al., 2012*** tested several variable selection methods, comparing PCA, siPLS, GA-PLS, UVE and CARS. A combinatorial method known as CARS-SPA (successive projections algorithm) was proposed to select variables from 678 wavelengths. The MLR model based on 27 selected wavelengths was developed to predict DM content with R^2p=0.86, and RMSEP=1.06%.

2.1.2 Internal and external defects

Discrimination between potato tuber and clods using HSI by detecting a significant wavebands was investigated by ***Al-Mallahi et al., 2008***. The intact potatoes were measured using a hyperspectral camera (SPECIM, ImSpector V10), in the range 321-1044 nm. The authors applied a machine vision system for optimum discrimination. It was found that the success rate of discrimination using one waveband at 480 nm was 98.8% under wet conditions, whereas another waveband at 752nm had a success rate of 94.7% under dry conditions. Two years later ***Al-Mallahi et al., 2010*** compared the previous discrimination and those by ultraviolet. The discrimination by UV showed the best results with 98.79% of the tubers, and 98.28% of the clods were detected successfully. The detection of common scab in potato was assessed by ***Dacal-Nieto et al., 2011*** using a spectrograph from Specim Imspector N17E (900-1700 nm). The authors developed Support Vector Machines (SVM) and Random Forest classifiers models based on spectra of 234 intact potatoes with different degrees of common scab incidence. The best results were obtained with the SVM classifier; they registered 97.1% accuracy to detect the percentage of the surface affected by common scab. ***Ray et al., 2011*** initially investigated the utility of reflectance HSI for potato late blight disease detection. The HSI data was collected for a potato crop at different levels of disease infestation in the range of 325 to 1075 nm and then Stepwise Discriminant Analysis was carried out to find out the most appropriate band to discriminate between different levels of infestation. The optimal hyperspectral wavebands to discriminate the healthy plants from disease infested plants were 540, 610, 620, 700, 710,730, 780 and 1040 nm; whereas up to 25% infestation could be discriminated using reflectance at 710, 720 and 750 nm.

Hu et al., 2016 tested HSI in order to determine the late blight in potato leaves. 60 potato leaves were used, 48 of them were vitro inoculated with pathogen of potato late blight, HSI data infected potato samples of different disease severity were acquired in 374 to 1018 nm and the least squares-support vector machine (LS-SVM) models were developed to discriminate healthy and affected potato leaves with 94.87% of accuracy. ***Franceschini et al., 2017*** also investigated the assessment of late blight (*Phytophthora infestans*) incidence on potato under organic cultivation. For this purpose, hyperspectral images were acquired during growing season by aerial pushbroom camera (WageningenUR Hyperspectral Mapping System) in the spectral range 450-915 nm. Results indicated that indices based on three spectral bands performed better and optimal wavelengths (i.e. near 490, 530 and 670 nm) are not only related to chlorophyll content but also to other leaf pigments like carotenoids.

Gao et al., 2012 used transmission hyperspectral imaging to detect internal black heart and external weight of potatoes. 266 images were collected in the spectral range 400-1000 nm. Only 9 wavelength Uninformative variable elimination (UVE) and successive projections algorithm (SPA) were applied to conduct the variable selection for the spectrum of the black heart samples. Then, PLSDA was applied to detect black heart with 9 selected wavelengths and a weight detection model by PLS. The results indicate that HSI transmission could be used to detect black heart with 100 % of accuracy (the minimum shoddy area which could be identified was 1.88 cm²) and weight with (Rp=0.99, RMSEP=10.88 g). ***Groinig et al.*** investigated the inline detection of sugar-end defects in potatoes. For this purpose, they used steam peeled potatoes; the images were acquired by HELIOS-EC3 NIR system (EVK DI Kerschhaggl GmbH/Raaba) in the wavelength range 900-1700 nm. The discrimination showed a good accuracy with 91.7 % of defects correctly classified using the EC3 prediction model.

The works of ***Huang et al., 2015*** made use of semi-transmission HSI combined with LSSVM algorithm to recognize internal and external defects in potatoes simultaneously. 315 potatoes from a farmers' market were used, and then HSI images were taken of normal external defects (bud and green rind) and internal defects (hollow heart). After that, the average spectrum was taken in the 390-1040 nm range. To reduce the dimensions of spectrum data including supervised locally linear embedding (SLLE), locally linear embedding (LLE) and isometric mapping (ISOMAP), the best results were obtained with SLLE-LSSVM and the single recognition rate of normal, bud, green rind and hollow heart potato reached 96.83%, 86.96%, 86.96% and 95% respectively. In another paper ***HUANG et al., (2015)*** conducted more in-depth research on detection of hollow heart by transmission HSI and competitive adaptive reweighed sampling algorithm (CARS) and successive projection algorithm (SPA) to select important variables. With 8 selected variables, the SVM model recognized hollow heart in potato with 94.64 % accuracy. This model was optimized by artificial fish swarm algorithm (AFSA), and then the recognition reached 100% of accuracy.

Jin et al., 2015 investigated the possibility of simultaneously distinguishing multiple defects by combined HSI and extreme learning machine (ELM). In this paper, 367 potatoes were picked which were made up of 111 sprouting potatoes, 90 green rind potatoes, 46 blackheart potatoes and 120 normal potatoes. The reflectance HSI images were acquired (SPECIM, V10E, Finland) in the wavelength range 390-1040 nm. Several models were tested. However the best models were obtained by using Diffusion maps (DM)-ELM model, the single recognition rate of sprouting potatoes, green rind potatoes, blackheart potatoes and normal potatoes respectively reached 97.30%, 93.55%, 94.44% and 100%, and the mixed recognition rate reached 96.58%.

HSI was investigated by ***López-Maestresalas et al., 2016*** to detect blackspot in the potato subsurface. 188 samples belonging to 3 different varieties were divided into two groups. Bruises were manually induced and samples were analyzed 1, 5, 9 and 24 h after bruising. The raw samples were analyzed in the reflectance Vis-NIR range 400-1000 nm and one for the SWIR range 1000-2500 nm using the ImSpector V10 (Spectral Imaging Ltd., Oulu, Finland) and HS SWIR XSM320C4-60 (Headwall Photonics Inc., Fitchburg, MA) cameras respectively. PCA, SIMCA and PLS-DA were used to build classifiers. The PLS-DA model achieved the better results above 94% for both hyperspectral setups. Furthermore, more accurate results were obtained with the SWIR setup at the tuber level (98.56 vs. 95.46% CC), enabling identification of early bruises within 5 h of bruising.

The paper of ***Noordam et al., 2005*** describes an application of both multispectral imaging and red/green/blue (RGB) color imaging for discriminating between different defect and diseases on raw French fries. Four different potato cultivars generally used for French fries production were selected from which fries are cut. The color images of the experiments were captured by a Sony 3-CCD color camera (www.sony.com), and the multispectral French fries images were recorded in 430-900 nm with an ImSpector V9 spectrograph (Spectral Imaging Ltd, Oulu, Finland). The modified snv preprocessed multispectral images and k-nearest neighbor's classifier (KNNC) give the best classification performance for raw RGB images. The detection of the latent greening defect in French fries with the exploration of multispectral images shows the additional value of multispectral imaging for French fries.

In the paper of ***Ye et al., 2018,*** the detection and classification of minor bruised potato were investigated.

Raw samples, including healthy and bruised potatoes belonging to 3 different levels (level I, II, and III bruises). In addition, the hyperspectral images were collected from 400 to 1000 nm by SOC710-VP portable visible light/near infrared (Vis-NIR) hyperspectral imager produced by Surface Optics Corporation, USA. In order to classify the bruise levels of bruised potatoes, two SVM models were established. The first one obtained the bruise recognition rate of 100% and the second one achieved a 100% success rate for the classification of bruised potatoes with level II and III. ***Zhou et al., 2011*** proposed a new method to detect external defects in the potato (dry rot, normal and other six kinds of common defect). PCA was used to classify defects of potatoes, the overall classification success rate was only 61.52%. In addition, band ratio algorithm and the symmetrical second difference algorithm were combined in order to improve classification accuracy, the success rate was increased to 95.65%.

In 2012 ***Zhou et al.,*** compared VIS-NIR diffuse reflectance and transmittance mode to detect black heart in potato. Reflectance and transmittance spectra were acquired using a hyperspectral image acquisition system, portable transmission spectrum acquisition system and FT-NIR spectrometer, respectively. The authors developed PLS-LDA model to classify the potatoes with or without black heart. Best results were obtained based on transmittance spectra with an accuracy of 98.46%. The works done by ***Zhou et al., 2016*** on two potato varieties to evaluate crop hail (damage levels of 0% (control), 33%, 66% and 99%) assessment by aerial multispectral imaging during two seasons. The images were collected 77 and 108 days after planting (0–60 days after damage) by using NiteCanon ELPH110 (LDP LLC, Carlstadt, NJ, USA) in the NIR range. Vegetation indices such as green normalized difference vegetation index (GNDVI), normalized difference vegetation index, and soil-adjusted vegetation index were calculated. The results showed 99% defoliation damage at the early bulk stage which also affected the crop yield significantly. Furthermore correlation analysis between vegetation indices and yield data indicated a strong relationship (r = 0.77–0.90) for damage at the early stage compared to other stages.

2.2 Banana

A few publications were found about HSI applied to banana characterization. They could be classified in two groups. (i) Quantification of chemical constituents and evaluation of physical properties such as maturity, firmness, color, moisture and total soluble solids. (ii) Evaluation of banana defects and diseases.

2.2.1 Chemical constituents and physical proprieties

Maturity stages, moisture content, firmness and total soluble solids were determined by ***Rajkumar et al., 2012*** at three different temperatures, viz., 20, 25, and 30 °C, and ripening stages from 1 to 6, with each group comprising 15 banana fruits, and using a hyperspectral imaging system spectrograph (ImSpector V10E, Optikon Co., Canada) in the spectral range 400-1000 nm. The Prediction model of Moisture content, TSS and firmness was developed by MLR on the optimal wavelengths with R^2 = 0.87, 0.85 and 0.91 respectively. In 2018 ***Xie et al.,*** investigated the feasibility of using HSI for determining banana color ($L*$, $a*$ and $b*$) and firmness as well as classifying ripe and unripe samples. The HSI images were acquired using an imaging spectrograph (V10E, Specim, Oulu, Finland), a charge coupled device (CCD) camera (C8484-05, Hamamatsu City, Japan) at wavelengths 380-1023 nm. PLS models were built to predict color and firmness. Based on the selected wavelengths, good results were obtained, with an Rp^2 of 0.795 for $L*$, 0.972 for $a*$, 0.773 for $b*$ and 0.760 for firmness. The corresponding residual predictive deviation (RPD) values were 2.234, 6.098, 2.119 and 2.062, respectively. The monitoring of the moisture, content, texture and color of banana slices during the drying process by using reflectance HSI was evaluated by **Nguyen-Do-Trong et al., 2018.** Thanks to a cross-polarized configuration the effects of glare or specular reflection on the banana slice surfaces in the hyperspectral diffuse reflectance images were greatly reduced. The data were collected at drying times of 0, 30, 60, 90, 120, 150, 180 and 210 mind by a hyperspectral system, which combined a CCD camera (TXG14NIR, Baumer, Switzerland), and spectrograph (V10 Specim, Finland) in the range 400-1000 nm. The PLSR calibration models were developed, and obtained very good results for water content (R^2P=0.97, RMSEP=0.05 kg water/kg DM), quite good results for and b*value (R^2P=0.83, RMSEP=1.95), and reasonable results for texture (R^2P=0.66, RMSEP=11.8 N), a* value (R^2P=0.53, RMSEP=1.32) and L* value (R^2P=0.61, RMSEP=5.92).

2.2.2 Defects and diseases

Wang et al., 2015 investigated the potential of HSI to predict the shelf life of bananas with different browning levels. Five optimal wavelengths (454, 486, 559, 686, and 728 nm) were selected by PCA. Then, image features and average spectra were used to develop classification models for determining their browning levels using back propagation (BP), radial basis function (RBF), and self-organizing feature maps (SOM) networks. BP classifier had the best performance with classification rates of 95.6 % for the training set and 90.5 % for the testing set, respectively. The work of ***Ochoa et al., 2016*** related to *in-vivo* detection of Black Sigatoka (BS) disease pre-symptomatic responses in banana leaves.

2.3 Cassava

Only one article was published on HSI applied to cassava. The goal of ***Su et al., 2017b*** was to detect cassava flour (CaF) adulterants in Irish organic wheat flour (OWF). Hyperspectral images (900–1700 nm) of OWF samples with a series of adulteration percentages were collected. PLSR and principal component regression (PCR) were employed for quantitative analysis. Feature wavelengths were selected from the loading plots of PCA, and from a first-derivative and mean centering iteration algorithm (FMCIA). The best model was developed using FMCIA. After, the corresponding feature wavelengths were further reduced based on model regression coefficients (RC). The optimal result of admixture detection was emerged by the RC-FMCIA-PLSR model, with R^2_P=0.973 and RMSEP=0.036 for OWF adulterated with CaF.

3 CONCLUSION

This literature review highlights the potential of Hyperspectral imaging (HSI) to qualify, sort and/or characterize roots, tubers or bananas. The techniques used vary in terms of complexity, accuracy, performances and robustness.

HSI covering ultra-violet, visible and/or NIR is one of the most recently emerging tools and provides the advantages of vision and spectroscopic systems; and can be used, after speeding up image acquisition time, for prediction of processing-related constituents as well as defects detection. HSI has the advantage of providing both quantification and information on spatial distributions of the traits in the whole tuber, root or banana. There is an inevitable trend for multispectral imaging with only a few important bands instead of full wavelengths in the non-destructive and rapid evaluation of food quality.

The research using HSI relates to fresh and processed products. Most of the time, quality control or process monitoring are achieved through the quantification of biochemical compounds: moisture content, nitrogen stress, sugars, solid soluble, volatile compounds, water blinding, dry matter, starch, acrylamide, protein, chlorophyll, water stress, soluble sugar and amino acid.

Another part of the research refers to internal and external defects such as black spot, scab detection, late blight sugar-end growth defects, bud and green rind, hollow heart, crop hail damage, bruising and brown streak disease. And some research focuses on physical proprieties such as specific gravity, cooking time, clods detection, weight, shape and firmness.

The products were analyzed in different conditions and presentations (intact, peeled, sliced, cooked, frying and chips). Regarding vision and spectroscopic techniques the measurements were taken in diffuse reflectance, transmittance or interactance mode using a static or moving sample holding systems. HIS measurements do not require contact with the sample and light levels are relatively high. However, spectral fingerprint is dependent on the skin properties of the tuber, in the case of intact tubers.

The chemometrics methods used to achieve calibration are numerous and depend on the product and on the trait to be characterized. The approaches cover linear methods (PCA, PCR, MLR, PLSR, LDA, PLSDA, SIMCA…) and non-linear methods (ANN, SVM, KNN, CARS...), and are divided into two groups: quantification and classification. In some cases classification (supervised or unsupervised) gives the opportunity to perform HTP screening, when quantification is not relevant.

4 REFERENCES

Al-Mallahi, A., Kataoka, T., and Okamoto, H. (2008). Discrimination between potato tubers and clods by detecting the significant wavebands. Biosyst. Eng. *100*, 329–337.

Al-Mallahi, A., Kataoka, T., Okamoto, H., and Shibata, Y. (2010). Detection of potato tubers using an ultraviolet imaging-based machine vision system. Biosyst. Eng. *105*, 257–265.

Amjad, W., Crichton, S.O.J., Munir, A., Hensel, O., and Sturm, B. (2018). Hyperspectral imaging for the determination of potato slice moisture content and chromaticity during the convective hot air drying process. Biosyst. Eng. *166*, 170–183.

Botha, E.J., Zebarth, B.J., and Leblon, B. (2006). Non-destructive estimation of potato leaf chlorophyll and protein contents from hyperspectral measurements using the PROSPECT radiative transfer model. Can. J. Plant Sci. *86*, 279–291.

Dacal-Nieto, A., Formella, A., Carrión, P., Vazquez-Fernandez, E., and Fernández-Delgado, M. (2011). Common Scab Detection on Potatoes Using an Infrared Hyperspectral Imaging System. In Image Analysis and Processing – ICIAP 2011, G. Maino, and G.L. Foresti, eds. (Springer Berlin Heidelberg), pp. 303–312.

Franceschini, M.H.D., Bartholomeus, H., van Apeldoorn, D., Suomalainen, J., and Kooistra, L. (2017). ASSESSING CHANGES IN POTATO CANOPY CAUSED BY LATE BLIGHT IN ORGANIC PRODUCTION SYSTEMS THROUGH UAV-BASED PUSHBROOM IMAGING SPECTROMETER. ISPRS - Int. Arch. Photogramm. Remote Sens. Spat. Inf. Sci. *XLII-2/W6*, 109–112.

Gao, H., Li, X., Xu, S., Huang, T., Tao, H., and Li, X. (2012). Transmission hyperspectral detection method for weight and black heart of potato.

Gerhards, M., Rock, G., Schlerf, M., and Udelhoven, T. (2016). Water stress detection in potato plants using leaf temperature, emissivity, and reflectance. Int. J. Appl. Earth Obs. Geoinformation *53*, 27–39.

Groinig, M., Burgstaller, M., and Pail, M. Industrial Application of a New Camera System based on Hyperspectral Imaging for Inline Quality Control of Potatoes. 8.

Hu, Y.H., Ping, X.W., Xu, M.Z., Shan, W.X., and He, Y. (2016). [Detection of Late Blight Disease on Potato Leaves Using Hyperspectral Imaging Technique]. Guang Pu Xue Yu Guang Pu Fen Xi Guang Pu *36*, 515–519.

Huang, T., Li, X.Y., Jin, R., Ku, J., Xu, S.M., Xu, M.L., Wu, Z.Z., and Kong, D.G. (2015). [Multi-Target Recognition of Internal and External Defects of Potato by Semi-Transmission Hyperspectral Imaging and Manifold Learning Algorithm]. Guang Pu Xue Yu Guang Pu Fen Xi Guang Pu *35*, 992–996.

HUANG, T., LI, X., XU, M., JIN, R., KU, J., XU, S., and WU, Z. (2015). Non-Destructive Detection Research for Hollow Heart of Potato Based on Semi-Transmission Hyperspectral Imaging and SVM.

Jin, R., Li, X., Yan, Y., Xu, M., Ku, J., Xu, S., and Hu, X. (2015). Detection method of multi-target recognition of potato based on fusion of hyperspectral imaging and spectral information.

Kjær, A., Nielsen, G., Stærke, S., Clausen, M.R., Edelenbos, M., and Jørgensen, B. (2016). Prediction of Starch, Soluble Sugars and Amino Acids in Potatoes (Solanum tuberosum L.) Using Hyperspectral Imaging, Dielectric and LF-NMR Methodologies. Potato Res. *59*, 357–374.

Kjær, A., Nielsen, G., Stærke, S., Clausen, M.R., Edelenbos, M., and Jørgensen, B. (2017). Detection of Glycoalkaloids and Chlorophyll in Potatoes (Solanum tuberosum L.) by Hyperspectral Imaging. Am. J. Potato Res. *94*, 573–582.

Liu, Y., Sun, Y., Xie, A., Yu, H., Yin, Y., Li, X., and Duan, X. (2017). Potential of Hyperspectral Imaging for Rapid Prediction of Anthocyanin Content of Purple-Fleshed Sweet Potato Slices During Drying Process. Food Anal. Methods *10*, 3836–3846.

López-Maestresalas, A., Keresztes, J.C., Goodarzi, M., Arazuri, S., Jarén, C., and Saeys, W. (2016). Non-destructive detection of blackspot in potatoes by Vis-NIR and SWIR hyperspectral imaging. Food Control *70*, 229–241.

Nguyen Do Trong, N., Tsuta, M., Nicolaï, B.M., De Baerdemaeker, J., and Saeys, W. (2011). Prediction of optimal cooking time for boiled potatoes by hyperspectral imaging. J. Food Eng. *105*, 617–624.

Nguyen-Do-Trong, N., Dusabumuremyi, J.C., and Saeys, W. (2018). Cross-polarized VNIR hyperspectral reflectance imaging for non-destructive quality evaluation of dried banana slices, drying process monitoring and control. J. Food Eng. *238*, 85–94.

Nigon, T.J., Mulla, D.J., Rosen, C.J., Cohen, Y., Alchanatis, V., and Rud, R. (2014). Evaluation of the nitrogen sufficiency index for use with high resolution, broadband aerial imagery in a commercial potato field. Precis. Agric. *15*, 202–226.

Nigon, T.J., Mulla, D.J., Rosen, C.J., Cohen, Y., Alchanatis, V., Knight, J., and Rud, R. (2015). Hyperspectral aerial imagery for detecting nitrogen stress in two potato cultivars. Comput. Electron. Agric. *112*, 36–46.

Noordam, J.C., Broek, W.H. van den, and Buydens, L.M. (2005). Detection and classification of latent defects and diseases on raw French fries with multispectral imaging. J. Sci. Food Agric. *85*, 2249–2259.

Ochoa, D., Cevallos, J., Vargas, G., Criollo, R., Romero, D., Castro, R., and Bayona, O. (2016). Hyperspectral imaging system for disease scanning on banana plants. In Sensing for Agriculture and Food Quality and Safety VIII, (International Society for Optics and Photonics), p. 98640M.

Rady, A.M., Guyer, D.E., Kirk, W., and Donis-González, I.R. (2014a). The potential use of visible/near infrared spectroscopy and hyperspectral imaging to predict processing-related constituents of potatoes. J. Food Eng. *135*, 11–25.

Rady, A.M., Guyer, D.E., Kirk, W., and Donis-González, I.R. (2014b). The potential use of visible/near infrared spectroscopy and hyperspectral imaging to predict processing-related constituents of potatoes. J. Food Eng. *135*, 11–25.

Rajkumar, P., Wang, N., Elmasry, G., Raghavan, G.S.V., and Gariepy, Y. (2012). Studies on banana fruit quality and maturity stages using hyperspectral imaging. J. Food Eng. *108*, 194–200.

Ray, S.S., Jain, N., Arora, R.K., Chavan, S., and Panigrahy, S. (2011). Utility of Hyperspectral Data for Potato Late Blight Disease Detection. J. Indian Soc. Remote Sens. *39*, 161.

Roosjen, P.P.J., Suomalainen, J.M., Bartholomeus, H.M., and Clevers, J.G.P.W. (2016). Hyperspectral Reflectance Anisotropy Measurements Using a Pushbroom Spectrometer on an Unmanned Aerial Vehicle—Results for Barley, Winter Wheat, and Potato. Remote Sens. *8*, 909.

Su, W.-H., and Sun, D.-W. (2016a). Multivariate analysis of hyper/multi-spectra for determining volatile compounds and visualizing cooking degree during low-temperature baking of tubers. Comput. Electron. Agric. *127*, 561–571.

Su, W.-H., and Sun, D.-W. (2016b). Potential of hyperspectral imaging for visual authentication of sliced organic potatoes from potato and sweet potato tubers and rapid grading of the tubers according to moisture proportion. Comput. Electron. Agric. *125*, 113–124.

Su, W.-H., and Sun, D.-W. (2017a). Chemical imaging for measuring the time series variations of tuber dry matter and starch concentration. Comput. Electron. Agric. *140*, 361–373.

Su, W.-H., and Sun, D.-W. (2017b). Evaluation of spectral imaging for inspection of adulterants in terms of common wheat flour, cassava flour and corn flour in organic Avatar wheat (Triticum spp.) flour - ScienceDirect.

Sun, H., Liu, N., Wu, L., Chen, L., Yang, L., Li, M., and Zhang, Q. (2018). Water Content Detection of Potato Leaves Based on Hyperspectral Image. IFAC-Pap. *51*, 443–448.

Sun, Y., Liu, Y., Yu, H., Xie, A., Li, X., Yin, Y., and Duan, X. (2017). Non-Destructive Prediction of Moisture Content and Freezable Water Content of Purple-Fleshed Sweet Potato Slices during Drying Process Using Hyperspectral Imaging Technique. Food Anal. Methods *10*, 1535–1546.

Wang, N.-N., Yang, Y.-C., Sun, D.-W., Pu, H., and Zhu, Z. (2015). Shelf-Life Prediction of 'Gros Michel' Bananas with Different Browning Levels Using Hyperspectral Reflectance Imaging. Food Anal. Methods *8*, 1173–1184.

Xie, C., Chu, B., and He, Y. (2018). Prediction of banana color and firmness using a novel wavelengths selection method of hyperspectral imaging. Food Chem. *245*, 132–140.

Yadav, A., Sengar, N., Issac, A., and Dutta, M.K. (2018). Image processing based acrylamide detection from fried potato chip images using continuous wavelet transform. Comput. Electron. Agric. *145*, 349–362.

Ye, D., Sun, L., Tan, W., Che, W., and Yang, M. (2018). Detecting and classifying minor bruised potato based on hyperspectral imaging. Chemom. Intell. Lab. Syst. *177*, 129–139.

Zhou, J., Pavek, M.J., Shelton, S.C., Holden, Z.J., and Sankaran, S. (2016). Aerial multispectral imaging for crop hail damage assessment in potato. Comput. Electron. Agric. *127*, 406–412.

Zhou, Z., Li, X., Tao, H., and Gao, H. (2011). Detection of potato external defects based onhyperspectral imaging technology.

Zhou, Z., Li, X., Gao, H., Tao, H., and Li, P. (2012). Comparison of diffuse reflection and transmission mode of visible/near infrared spectroscopy for detecting black heart of potato.

Su, W.-H., and Sun, D.-W. (2017). Evaluation of spectral imaging for inspection of adulterants in terms of common wheat flour, cassava flour and corn flour in organic Avatar wheat (Triticum spp.) flour - ScienceDirect.

Institution: Cirad – UMR QualiSud

Address: C/O Cathy Méjean, TA-B95/15 - 73 rue Jean-François Breton - 34398 MONTPELLIER Cedex 5 - France

Contact Tel: +33 4 67 61 44 31

Contact Email: rtbfoodspmu@cirad.fr